Phosphorescence of C 5 N − in Rare Gas Solids

Urszula Szczepaniak, Robert Kolos, Jean-Claude Guillemin, Claudine Crépin

photochem

MDPI

Article

Phosphorescence of C_5N^- in Rare Gas Solids

Urszula Szczepaniak [1,2,†], Robert Kołos [2,*], Jean-Claude Guillemin [3] and Claudine Crépin [1,*]

[1] Institut des Sciences Moléculaires d'Orsay (ISMO), CNRS, Université Paris-Saclay, F-91405 Orsay, France; u.szczepaniak@obviotec.com
[2] Institute of Physical Chemistry, Polish Academy of Sciences, Kasprzaka 44/52, PL-01-224 Warsaw, Poland
[3] Ecole Nationale Supérieure de Chimie de Rennes, CNRS, Univ. Rennes, ISCR–UMR6226, F-35000 Rennes, France; jean-claude.guillemin@ensc-rennes.fr
* Correspondence: rkolos@ichf.edu.pl (R.K.); claudine.crepin-gilbert@universite-paris-saclay.fr (C.C.); Tel.: +48-22-343-32-18 (R.K.); +33-1-69-15-75-39 (C.C.)
† Current address: obvioTec AG, Garstligweg 8, 8634 Hombrechtikon, Switzerland.

Abstract: Phosphorescence of C_5N^- was discovered following the ArF-laser (193 nm) photolysis of cyanodiacetylene (HC_5N) isolated in cryogenic argon, krypton, and xenon matrices. This visible emission, with an origin around 460 nm, is vibrationally resolved, permitting the measurement of frequencies for eight ground-state fundamental vibrational modes, including the three known from previous IR absorption studies. Phosphorescence lifetime amounts to tens or even hundreds of ms depending on the matrix host; it is five times longer than in the case of HC_5N.

Keywords: anion; cyanopolyyne; luminescence; matrix isolation

Citation: Szczepaniak, U.; Kołos, R.; Guillemin, J.-C.; Crépin, C. Phosphorescence of C_5N^- in Rare Gas Solids. *Photochem* **2022**, *2*, 263–271. https://doi.org/10.3390/photochem2020019

Academic Editor: Elena Cariati

Received: 14 February 2022
Accepted: 22 March 2022
Published: 28 March 2022

1. Introduction

Cyanopolyynes ($HC_{2n+1}N$) constitute the most prominent homologous series of astrochemically-relevant molecules. They have been detected via microwave rotational transitions in many extraterrestrial sources, up to $n = 5$ [1–7]. Cyanopolyyne radicals $C_{2n+1}N$ and the corresponding anions $C_{2n+1}N^-$ ($n = 1, 2$) have also been identified in the interstellar medium [8,9]. The first detection of C_5N^-, in microwave emission from the shell of a carbon star IRC +10216, was based solely on theoretical spectroscopic predictions, as no laboratory data existed. The anion may also be present in Titan's atmosphere [10].

Vibrational spectroscopy of C_3N^- and C_5N^- generated from HC_3N and HC_5N in rare gas solids was studied via IR absorption [11,12]. IR photodissociation spectroscopy provided information on certain stretching modes for gas-phase $C_{2n+1}N^-$ ($n = 1$ to 5) species [13]. Ultraviolet and visible absorption was studied for these anions ($n = 3$ to 6) in solid neon [14].

Photoelectron spectroscopy of C_3N^- and C_5N^- supplied the adiabatic electron detachment energies as high as 4.305 ± 0.001 and 4.45 ± 0.03 eV, respectively [15]. These values, measured for gas-phase species, are expected to be even higher for anions isolated in rare-gas cryogenic matrices, given that polarizable media better stabilize a charged species than a neutral one. For C_3^- and C_6^-, in solid Ar, the measured photodetachment thresholds were, respectively, 0.24 and 0.48 eV higher than in the gas phase [16]. For C_8H^- in Ne, absorption to a valence state located 0.39 eV above the gas-phase photodetachment energy was reported [14].

The most extensive theoretical study dealing with the ground electronic state characteristics of $C_{2n+1}N^-$ species (including the vertical electron detachment energies) was published by Botschwina and Oswald in 2008 [17]. More recently, Skomorowski et al. [18] provided reliable (EOM-CCSD) predictions for the energies of vertical excitations to the bound electronic states of $n = 0$ to 3 species, and for the resonances embedded in continua above the ground states of the corresponding neutral radicals.

Phosphorescence has already been observed for C_3N^- anion produced by UV irradiation of Ar, Kr, and Xe matrices doped with HC_3N [19]. Here we report on similar experiments aimed at C_5N^-, carried out with HC_5N-doped rare gas matrices.

2. Experimental

The precursor molecule, HC_5N, was synthesized using the method developed by Trolez and Guillemin [20] and purified before each experiment by exposing to vacuum at T ≈ 200 K.

Noble gas (hereafter: NG; Ar 4.5, Kr 4.0 or Xe 4.8 from Messer) was mixed with precursor molecules at a ratio of approx. 500:1, using standard manometric techniques. The mixture was subsequently trapped inside the closed-cycle helium refrigerator (Air Products Displex DE202FF, CaF_2 windows) onto a sapphire plate at 22 K (Ar), 30 K (Kr), or 14 K (Xe) as measured and regulated with a Scientific Instruments Inc. 9620-1 temperature controller. The typical amount of deposited gas was 6–8 mmol. All spectroscopic measurements were carried out at the lowest attainable temperature, 7–8 K. Composition of the samples was verified with a Nicolet FTIR spectrometer, either Nexus 670/870 or iS50 (resolution of 0.125 cm^{-1}), equipped with liquid nitrogen-cooled MCT detectors. The use of a sapphire substrate plate imposed the low-frequency detection limit of approx. 1350 cm^{-1}. Cryogenic samples were photolyzed with a 193 nm ArF excimer laser (Coherent Compex Pro), during or after the sample deposition. The laser typically operated at a repetition rate of 10 Hz, the energy delivered to the sample surface did not exceed 5 mJ/cm^2 per pulse, and the usual irradiation time was several hours (at least 4 h in Ar, 3 h in Kr and 1 h in Xe).

A Continuum Surelite II + OPO Horizon pulse laser system operating at 10 Hz in the 192–400 nm range was used for the excitation of luminescence. That latter was dispersed with a 0.6 m Jobin-Yvon grating monochromator and detected either with a photomultiplier (Hamamatsu H3177-50) connected to the exit slit or with a gated CCD camera (Andor iStar DH720), both featuring a detection range of 200–850 nm. Time synchronization between excitation pulses and luminescence detection was provided by a home-made triggering device. Tunable excitation permitted us to separate the new emission features from those of the already known phosphorescence of the parent molecule [21] or of the chain-growth products [22].

In luminescence decay time measurements, phosphorescence light, selected with the grating monochromator, was detected by the photomultiplier. Photons arriving after the excitation laser pulse were counted in successive time gates using a National Instrument acquisition card (PCIe-6251) and a homemade LabView-based software.

3. Results and Discussion

Strong phosphorescence of HC_5N in NG solids was discovered and analyzed in the course of our previous studies [21]. The UV photolysis of that compound trapped in Ar led to the isoelectronic anion C_5N^- detected via its IR spectrum [12]. On the other hand, phosphorescence of C_3N^- was found in photolyzed NG matrices doped with HC_3N [19]. We therefore sought to find phosphorescence of C_5N^- by photolyzing HC_5N. The ArF laser radiation (193 nm) was applied. The choice of optimal conditions to photoexcite the anion was crucial, given that the parent species phosphoresces and that the presence of an intensely emitting photoproduct (dicyanooctatetrayne, $NC_{10}N$) in irradiated HC_5N/NG samples was previously reported [22].

Four major new luminescence bands appeared in a correlated way after UV irradiation in all three applied noble gas matrices. Their frequencies are listed in Table 1. This vibrationally structured emission was distinctly different from the phosphorescence of either the precursor molecule [21] or of $NC_{10}N$ [22]. It is recognized as the phosphorescence of C_5N^- based on the following arguments: (i) analysis of its vibronic structure reveals three stretching fundamental frequencies of C_5N^- that were independently measured via IR absorption (see Table 1); (ii) it is long-lived, in the millisecond time range; and (iii) its

origin (2.68–2.69 eV) conforms to the vertical singlet-triplet excitation energy (3.03 eV) theoretically predicted for C_5N^- [18].

Table 1. Vibronic band wavenumbers ($\tilde{\nu}$) of C_5N^- phosphorescence, as measured in noble gas matrices. Resultant distances from the vibrationless phosphorescence origin ($\Delta\tilde{\nu}$) are juxtaposed with IR absorption data ($\tilde{\nu}_{IR}$), when available. All values in cm^{-1}; the estimated error of ($\Delta\tilde{\nu}$) is 8 cm^{-1}.

Ar			Kr		Xe			Involved Mode
$\tilde{\nu}$	$\Delta\tilde{\nu}$	$\tilde{\nu}_{IR}$ [1]	$\tilde{\nu}$	$\Delta\tilde{\nu}$	$\tilde{\nu}$	$\Delta\tilde{\nu}$	$\tilde{\nu}_{IR}$	
21,720			21,721/21,697		21,614			
~19,800	1920	1923.2	19,798/19,767	1923/1930	19,692	1922	1925.4	ν_1
19,610	2110	2111.3	19,610/19,577	2111/2120	19,505	2109	2119.1	ν_2
19,540	2180	2183.8	19,543/19,510	2178/2187	19,428	2186	2191.2	ν_3

[1] Ref. [12].

Said emission could be detected, with varying intensity, following the excitation in a large spectral range (370–220 nm). Phosphorescence intensity depended also on the matrix material, being the highest in solid Xe and the lowest in solid Ar. Photon energies in the vicinity of 3.6 eV were chosen for efficient luminescence excitation in Kr and Xe. Such radiation should excite only the C_5N^- emission (via $1^1\Sigma^-$ or $1^1\Delta$ states) [18] and guaranteed the avoidance of electron detachment. In Ar, phosphorescence of C_5N^- was difficult to detect; it was better seen with more energetic excitation (e.g., 287 nm (4.32 eV)).

Figure 1 shows the main emission bands assigned to C_5N^-, observed in various NG matrices. The spectral features detected in Ar were very weak and broad. The highest energy one, with a structure due to multiple trapping sites, can be seen as the dotted line in Figure 1. In Kr (bottom panel of Figure 1), the origin band appeared as a doublet around 21,700 cm^{-1} and two dominant components were also observed in the remaining bands, the anion therefore seems to be trapped in two main matrix sites. Conversely, phosphorescence detected in Xe (top panel) exhibited single, narrow bands, which allowed for clear assignments of the vibronic structure.

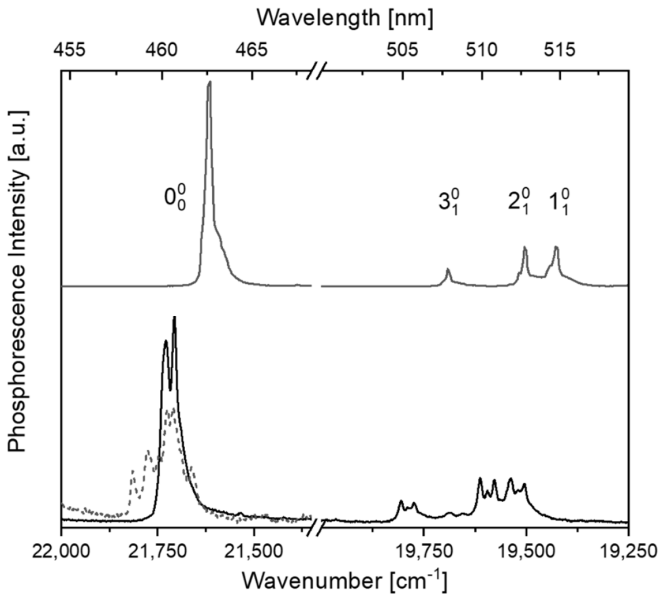

Figure 1. Laser-excited phosphorescence of C_5N^-, as detected in photolyzed (193 nm) NG matrices doped with HC_5N, T = 8 K. Top: Xe matrix, excitation 349.5 nm (3.55 eV, 28,610 cm^{-1}). Bottom, continuous line: Kr matrix, excitation 347.1 nm (3.57 eV, 28,810 cm^{-1}). Dotted line: in Ar matrix, excitation 287 nm (4.32 eV, 34,840 cm^{-1}).

A thorough vibronic analysis of phosphorescence was possible in solid Xe, where the high signal-to-noise ratio gave access to a multitude of weak emission lines. Figure 2 shows the full phosphorescence spectrum (the origin band appears as saturated in order to reveal the weakest features). The assignment of observed bands, reported in Table 2, was assisted with theoretical predictions [12,17]. A comparison of the vibrational frequencies deduced from the phosphorescence spectrum and those theoretically predicted is reported in Table 3.

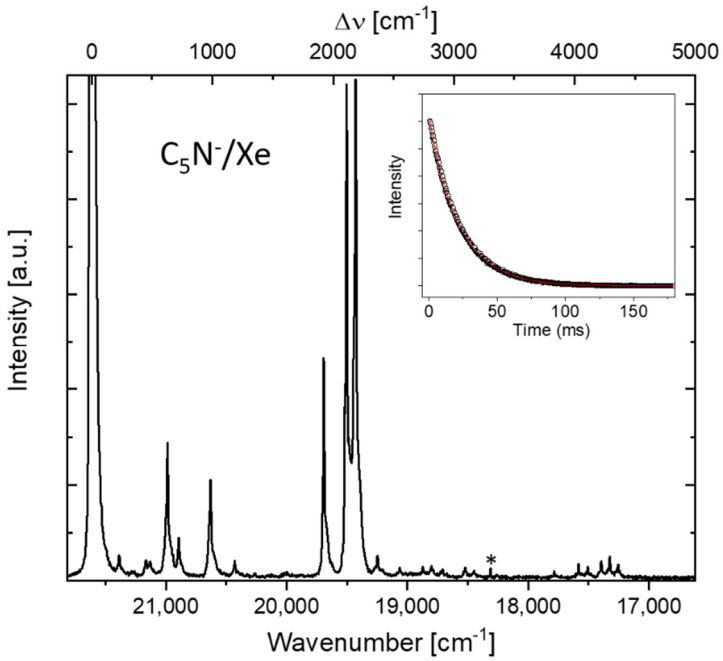

Figure 2. Laser-excited (349.5 nm) phosphorescence of C_5N^-, as detected in a photolyzed (193 nm) HC_5N/Xe matrix, T = 8 K (vertical expansion of the top trace of Figure 1). Asterisk marks an Hg line used for wavelength calibration. Insert: C_5N^- phosphorescence decay in Xe; emission detected at 21,615 cm^{-1}. Red trace shows the monoexponential fitting curve with a time constant of 21.94 ± 0.03 ms.

Table 2. Wavelengths (λ, nm), wavenumbers ($\tilde{\nu}$, cm^{-1}), and assignments of vibronic bands for the a $^3\Sigma$–X $^1\Sigma^+$ system of C_5N^- anion isolated in solid Xe. Relative values ($\Delta\tilde{\nu}$, cm^{-1}) give distances from the vibrationless origin.

λ	$\tilde{\nu}$	$\Delta\tilde{\nu}$	Intensity [1]	Assignment
462.7	21,614	0	*vvs*	0_0^0
467.5	21,388	226	*vw*	8_1^0 (or 9_2^0)
470.4	21,279	335	*vvw*	$8_1^0 9_1^0$
472.5	21,164	450	*vw*	8_2^0 (or 9_4^0)
473.3	21,130	484	*vw*	7_1^0
476.5	20,985	629	*m*	5_1^0
478.6	20,893	721	*w*	$7_1^0 8_1^0$
484.8	20,629	985	*m*	7_2^0
489.5	20,429	1184	*vw*	4_1^0
507.8	19,692	1922	*s*	3_1^0
512.7	19,505	2109	*vs*	2_1^0
514.7	19,428	2185	*vs*	1_1^0
519.6	19,246	2368	*vw*	4_2^0
524.6	19,063	2551	*vvw*	$3_1^0 5_1^0$
530.0	18,869	2744	*vvw*	$2_1^0 5_1^0$
531.9	18,799	2815	*vvw*	$1_1^0 5_1^0$
534.5	18,707	2906	*vvw*	$3_1^0 7_2^0$

Table 2. *Cont.*

λ	$\tilde{\nu}$	$\Delta\tilde{\nu}$	Intensity [1]	Assignment
540.0	18,520	3094	*vvw*	$2_1^0 7_2^0$
542.1	18,447	3167	*vvw*	$1_1^0 7_2^0$
562.3	17,784	3830	*vvw*	3_2^0
568.8	17,582	4032	*vw*	$2_1^0 3_1^0$
571.3	17,505	4109	*vw*	$1_1^0 3_1^0$
574.9	17,394	4220	*vw*	2_2^0
577.2	17,324	4290	*vw*	$1_1^0 2_1^0$
579.6	17,252	4361	*vw*	1_2^0

[1] *s*: strong, *m*: medium, *w*: weak, *v*: very.

Table 3. Wavenumbers of fundamental vibrational modes for C_5N^- anion. All values in cm^{-1}.

Mode, Symmetry	Theory		Experiment	
	DFT [1]	CCSD(T) [2]	Ar Matrix [3]	Xe Matrix [4]
ν_1 σ	2184	2202.6	2183.8	2186
ν_2 σ	2116	2128.6	2111.3	2109
ν_3 σ	1921	1927.2	1923.2	1922
ν_4 σ	1166	1167.7		1184
ν_5 σ	612	614.4		629
ν_6 π	529	503.0		
ν_7 π	500	493.7		484
ν_8 π	242	227.4		226
ν_9 π	102	96.5		109 [5]

[1] Harmonic values scaled by 0.96, basis set aug-cc-pVTZ (Ref. [12]). [2] Basis set cc-pVQZ+, anharmonic calculations of stretching modes and harmonic calculations of bending modes (Ref. [17]). [3] IR absorption measurement (Ref. [12]). [4] This work, derived from electronic phosphorescence. [5] Tentative, based on a combination mode $8_1^0 9_1^0$.

The most intense vibronic bands in C_5N^- phosphorescence are those due to the fundamental modes associated with triple bonds, namely ν_1, ν_2, and ν_3 (it should be noted that the shorter chain of C_3N^- has just two alike modes with frequencies around 2000 cm^{-1}; both were shown to dominate in its triplet-singlet emission [19]). In phosphorescence of other previously studied mono- [21,23–25] and dicyanopolyyne [22,26–28] molecules, the vibronic bands produced by the triple bonds were also prominent. The mode contributing especially strongly to the vibronic structure of these emissions was a stretching, either a quasi-centrosymmetric one for the $C_{2n+1}N$ backbone [24] or fully symmetric for $NC_{2n}N$ [22], which caused, along the chain, shrinking of the consecutive interatomic distances alternated with their expansion (i.e., an in-phase oscillation of the three triple bonds) [29]. Distortion patterns of that type qualitatively resembled the geometry changes predicted to accompany the $a^3\Sigma^+$–$X^1\Sigma^+$ transitions of cyanopolyyne-family molecules, including C_5N^- [29]. For the latter species, however, there is no vibrational mode around 2000 cm^{-1} that would produce the unison expansion or the unison shrinking of all triple bonds. Still, such an in-phase distortion of two triple bonds is the characteristic shared by the crucial modes ν_1, ν_2, and ν_3.

The two remaining stretching fundamentals ν_4 and ν_5 (influenced mostly by distortions of the single C-C bonds), are also clearly visible in the vibronic structure (at 1184 cm^{-1} and 629 cm^{-1}, respectively; see Figure 2, Table 2). The quasi-symmetric mode ν_5 is similar to the C-C stretch-related bands observed in phosphorescence of HC_5N (ν_6) [21] or C_4N_2 (ν_3, *gerade* symmetry) [26]. The band due to ν_4 is weak but unambiguously assigned. It is noteworthy that its analogues were revealed only as overtones in phosphorescence of C_4N_2 and HC_5N. Bending (π-symmetry) modes appear weakly in phosphorescence due to its Σ^+–Σ^+ orbital character. The ν_8 band at 226 cm^{-1} is easily assigned by comparison with theoretical values (Table 3) and taking into account that similar modes were identified in phosphorescence spectra of HC_5N [21] and C_4N_2 [26]. A frequency of 109 cm^{-1} can

be deduced for the lowest-energy bending (ν_9) based on a very weak feature tentatively recognized as a combination band. Another bending-related band appears at 484 cm^{-1}. It is assigned to ν_7 based on theoretical predictions (Table 3). The highest-energy bending (*zig-zag* type, ν_6) does not seem to produce a detectable vibronic band. Nonetheless, such a mode appeared, albeit weakly, in phosphorescence of HC_5N [21], C_4N_2 [26] and C_3N^- [19]. Considering the closeness of ν_6 and ν_7 (separation of 9 cm^{-1} derived with harmonic CCSD(T) calculations) [17], a possibility exists, however, that the band at 484 cm^{-1} represents the said *zig-zag* mode and ν_7 is not detected.

Present non-detection of IR absorption bands for C_5N^- generated in Ar or Kr matrices indicates that 193 nm laser radiation was not as effective in producing this anion as the broadband far-UV irradiation applied by Coupeaud et al. [12]. In solid Xe, however, IR bands due to ν_1, ν_2, and ν_3 stretching fundamentals of C_5N^- could be discerned (see Table 1). Some mismatch between $\Delta\widetilde{\nu}$ and $\widetilde{\nu}_{IR}$ values listed in Table 1 may stem, on the one hand, from the experimental error inherent to $\Delta\widetilde{\nu}$ (5–8 cm^{-1}) and, on the other hand, from the coupling of the electronic transition with phonons. That last issue is mode-specific and may slightly deviate the maximum of the measured phosphorescence bands from the true zero-phonon transition frequencies.

Influence of the NG environment is manifested by a red-shift of phosphorescence in Xe, with respect to Kr. It is usual for the transitions involving valence electrons and originates from an increase of the host polarizability. Furthermore, the size of C_5N^- is obviously bigger than the distance between the nearest NG atoms forming the lattice, which may induce the trapping of HC_5N and C_5N^- in multiple sites. This is indeed observed in Ar and Kr, but not in Xe, where the lattice parameter is the largest.

A very long luminescence decay time was evident even to the naked eye. As reported for numerous instances of triplet-singlet transitions in NG matrices (see e.g., Ref. [30]), the heavier the host, the shorter the phosphorescence decay (we observed the same pattern for the related, matrix-isolated molecules HC_5N [21] and C_4N_2 [26]). This is a consequence of the spin-orbit coupling enhancement by external heavy atoms [31–33]. The values presently measured in Kr and Xe matrices are, respectively, ~250 ms and ~22 ms (see the insert of Figure 2). These are ca. five times higher than those of the isoelectronic species HC_5N (~50 ms in Kr and ~4.8 ms in Xe, as presently measured in the same samples). It indicates a much lower nonradiative $T_1 \rightarrow S_0$ conversion efficiency for C_5N^- than for HC_5N, in possible relation to an intersystem crossing channel enhanced by the presence of large CH stretching mode energy quanta. Phosphorescence lifetime reported for the shorter analogue, C_3N^-, was twice as long (~0.5 s in Kr) [19], likely due to a smaller number of internal degrees of freedom, leading to less efficient non-radiative relaxation. Such a decrease in the phosphorescence lifetime with the increase of polyynic chain length was pointed out in our previous reports on mono- and dicyanopolyynes [22,29].

The detection of photoproducts in UV-irradiated HC_5N/NG samples, including cyanodiacetylene isomers [12], intermolecular coupling products (HC_9N [24], $C_{10}N_2$ [22]), and noble gas insertion species H-NG-C_5N [34], is already well documented. While we do not provide here any in-depth discussion of the energetics of C_5N^- formation from HC_5N, it should be noted that a gas-phase process leading from that precursor to H^+ and C_5N^- would require an overall energy input by far higher than that provided with a single quantum of 193 nm radiation. However, one should consider that (i) C_5N radicals are being formed in the sample (as elucidated from the kinetics of the parallel production of $NC_{10}N$ [22]), (ii) electron attachment to these radicals is obviously exothermic, and (iii) protons, when bound as NG-H-NG^+ cations, can be stabilized in NG matrices [35]. The latter species could not be traced in the present experiments, due to the use of a sapphire substrate plate (see Experimental). However, Ar_2H^+ cations were shown to accompany C_5N^- in a correlated manner when HC_5N was photolyzed in solid argon [12]. Importantly, we did not observe any trace of C_5N^- in a sample deprived of noble gas atoms, i.e., when dinitrogen was used as a host material for HC_5N photolysis.

The $a^3\Sigma^+$–$X^1\Sigma^+$ system of C_5N^- could be induced with wavelengths from a broad range, approx. 370–200 nm. A detailed study of phosphorescence excitation spectra is in progress, together with the relevant theoretical support. Especially interesting are the relaxation pathways leading to the observed emission when excitation energy exceeds the C_5N^- photodetachment threshold.

4. Conclusions

Phosphorescence of C_5N^- was observed here for the first time. Lifetime of the involved lowest triplet state is five times longer than for the parent HC_5N molecule. Positions of the main vibronic bands of the $a^3\Sigma^+$–$X^1\Sigma^+$ system are consistent with the frequencies of the three vibrational modes previously observed [12] in IR absorption spectra. Matrix material, either Ar, Kr, or Xe, was shown to influence both the intensity of phosphorescence and its band structure. In particular, the presence of two main matrix sites (types of microenvironments) is suggested by the doubling of bands observed in Kr, whereas the Xe-matrix spectra seem to originate in a single site. Phosphorescence characteristics, influenced by the external heavy atom effect, did not show any measurable site-dependence in Kr, while the host dependence (Xe vs. Kr) was obvious in terms of both emission intensity and decay time. Emission from the Xe matrix sample, intense and rich in detail, allowed for the first measurement of the previously unreachable ground-state vibrational frequencies ν_4, ν_5, ν_7, ν_8, and (tentatively) ν_9.

Author Contributions: Conceptualization, R.K. and C.C.; methodology, R.K. and C.C.; formal analysis, U.S., R.K. and C.C.; investigation, U.S. and R.K.; resources, J.-C.G. and C.C.; writing—original draft preparation, U.S., R.K. and C.C.; writing—review and editing, U.S., R.K., J.-C.G. and C.C.; supervision, R.K. and C.C.; funding acquisition, U.S., R.K., J.-C.G. and C.C. All authors have read and agreed to the published version of the manuscript.

Funding: This work was financially supported by the Polish National Science Centre, project no. 2011/03/B/ST4/02763, French-Polish scientific cooperation programs Partenariat Hubert-Curien Polonium (2012–2013) and PICS (2014–2016). U.S. is a beneficiary of the French Government scholarship Bourse Eiffel, managed by Campus France, and of the project "Scholarships for PhD students of Podlaskie Voivodeship". The project is co-financed by European Social Fund, Polish Government and Podlaskie Voivodeship. J.-C.G. thanks for the financial support received from Centre National d'Etudes Spatiales (CNES) and the French program Physique et Chimie du Milieu Interstellaire (PCMI) funded by the Centre National de la Recherche Scientifique and CNES.

Institutional Review Board Statement: Not applicable.

Data Availability Statement: The data presented in this study are available within the article.

Acknowledgments: We thank Michèle Chevalier for assistance in experiments and Marcin Gronowski for the discussion of theoretical issues.

Conflicts of Interest: The authors declare no conflict of interest.

References

1. Turner, B.E. Detection of Interstellar Cyanoacetylene. *Astrophys. J. Lett.* **1971**, *163*, L35–L39. [CrossRef]
2. Mauersberger, R.; Henkel, C.; Sage, L.J. Dense Gas in Nearby Galaxies. III-HC_3N as an Extragalactic Density Probe. *Astron. Astrophys.* **1990**, *236*, 63–68.
3. Kunde, V.G.; Aikin, A.C.; Hanel, R.A.; Jennings, D.E.; Maguire, W.C.; Samuelson, R.E. C_4H_2, HC_3N and C_2N_2 in Titan's Atmosphere. *Nature* **1981**, *292*, 686–688. [CrossRef]
4. Bockelée-Morvan, D.; Lis, D.C.; Wink, J.E.; Despois, D.; Crovisier, J.; Bachiller, R.; Benford, D.J.; Biver, N.; Colom, P.; Davies, J.K.; et al. New Molecules Found in Comet C/1995 O1 (Hale-Bopp): Investigating the Link between Cometary and Interstellar Material. *Astron. Astrophys.* **2000**, *353*, 1101–1114.
5. Snell, R.L.; Schloerb, F.P.; Young, J.S.; Hjalmarson, A.; Friberg, P. Observations of HC_3N, HC_5N, and HC_7N in Molecular Clouds. *Astrophys. J.* **1981**, *244*, 45. [CrossRef]
6. Broten, N.W.; Oka, T.; Avery, L.W.; MacLeod, J.M.; Kroto, H.W. The Detection of HC_9N in Interstellar Space. *Astrophys. J.* **1978**, *223*, L105–L107. [CrossRef]

7. Loomis, R.A.; Burkhardt, A.M.; Shingledecker, C.N.; Charnley, S.B.; Cordiner, M.A.; Herbst, E.; Kalenskii, S.; Lee, K.L.K.; Willis, E.R.; Xue, C.; et al. An Investigation of Spectral Line Stacking Techniques and Application to the Detection of $HC_{11}N$. *Nat. Astron.* **2021**, *5*, 188–196. [CrossRef]
8. Thaddeus, P.; Gottlieb, C.A.; Gupta, H.; Brünken, S.; McCarthy, M.C.; Agúndez, M.; Guélin, M.; Cernicharo, J. Laboratory and Astronomical Detection of the Negative Molecular Ion C_3N^-. *Astrophys. J.* **2008**, *677*, 1132–1139. [CrossRef]
9. Cernicharo, J.; Guélin, M.; Agúndez, M.; McCarthy, M.C.; Thaddeus, P. Detection of C_5N^- and Vibrationally Excited C6H in IRC +10216. *Astrophys. J.* **2008**, *688*, L83–L86. [CrossRef]
10. Vuitton, V.; Lavvas, P.; Yelle, R.V.; Galand, M.; Wellbrock, A.; Lewis, G.R.; Coates, A.J.; Wahlund, J.E. Negative Ion Chemistry in Titan's Upper Atmosphere. *Planet. Space Sci.* **2009**, *57*, 1558–1572. [CrossRef]
11. Kołos, R.; Gronowski, M.; Botschwina, P. Matrix Isolation IR Spectroscopic and Ab Initio Studies of C_3N^- and Related Species. *J. Chem. Phys.* **2008**, *128*, 154305. [CrossRef] [PubMed]
12. Coupeaud, A.; Turowski, M.; Gronowski, M.; Piétri, N.; Couturier-Tamburelli, I.; Kołos, R.; Aycard, J.P. C_5N^- Anion and New Carbenic Isomers of Cyanodiacetylene: A Matrix Isolation IR Study. *J. Chem. Phys.* **2008**, *128*, 154303. [CrossRef] [PubMed]
13. Stanca-Kaposta, E.C.; Schwaneberg, F.; Fagiani, M.R.; Wende, T.; Hagemann, F.; Wünschmann, A.; Wöste, L.; Asmis, K.R. Infrared Photodissociation Spectroscopy of $C_{2n+1}N^-$ Anions with n = 1–5. *Z. Phys. Chem.* **2014**, *228*, 351–367. [CrossRef]
14. Grutter, M.; Wyss, M.; Maier, J.P. Electronic Absorption Spectra of $C_{2n}H^-$, $C_{2n-1}N^-$ (n = 4–7), and $C_{2n-1}N$ (n = 3–7) Chains in Neon Matrices. *J. Chem. Phys.* **1999**, *110*, 1492–1496. [CrossRef]
15. Yen, T.A.; Garand, E.; Shreve, A.T.; Neumark, D.M. Anion Photoelectron Spectroscopy of C_3N^- and C_5N^-. *J. Phys. Chem. A* **2010**, *114*, 3215–3220. [CrossRef] [PubMed]
16. Szczepanski, J.; Ekern, S.; Vala, M. Vibrational Spectroscopy of Small Matrix-Isolated Linear Carbon Cluster Anions. *J. Phys. Chem. A* **1997**, *101*, 1841–1847. [CrossRef]
17. Botschwina, P.; Oswald, R. Carbon Chains of Type $C_{2n+1}N^-$ (N = 2–6): A Theoretical Study of Potential Interstellar Anions. *J. Chem. Phys.* **2008**, *129*, 044305. [CrossRef]
18. Skomorowski, W.; Gulania, S.; Krylov, A.I. Bound and Continuum-Embedded States of Cyanopolyyne Anions. *Phys. Chem. Chem. Phys.* **2018**, *20*, 4805–4817. [CrossRef]
19. Turowski, M.; Gronowski, M.; Boyé-Péronne, S.; Douin, S.; Moneron, L.; Crépin, C.; Kołos, R. The C_3N^- Anion: First Detection of Its Electronic Luminescence in Rare Gas Solids. *J. Chem. Phys.* **2008**, *128*, 164304. [CrossRef] [PubMed]
20. Trolez, Y.; Guillemin, J.-C. Synthesis and Characterization of 2,4-Pentadiynenitrile—A Key Compound in Space Science. *Angew. Chem. Int. Ed.* **2005**, *44*, 7224–7226. [CrossRef] [PubMed]
21. Turowski, M.; Crépin, C.; Gronowski, M.; Guillemin, J.C.; Coupeaud, A.; Couturier-Tamburelli, I.; Pietri, N.; Kołos, R. Electronic Absorption and Phosphorescence of Cyanodiacetylene. *J. Chem. Phys.* **2010**, *133*, 074310. [CrossRef]
22. Szczepaniak, U.; Kołos, R.; Gronowski, M.; Chevalier, M.; Guillemin, J.C.; Crépin, C. Synthesis and Electronic Phosphorescence of Dicyanooctatetrayne ($NC_{10}N$) in Cryogenic Matrixes. *J. Phys. Chem. A* **2018**, *122*, 5580–5588. [CrossRef]
23. Couturier-Tamburelli, I.; Piétri, N.; Crépin, C.; Turowski, M.; Guillemin, J.C.; Kołos, R. Synthesis and Spectroscopy of Cyanotriacetylene (HC7N) in Solid Argon. *J. Chem. Phys.* **2014**, *140*, 044329. [CrossRef] [PubMed]
24. Szczepaniak, U.; Kołos, R.; Gronowski, M.; Chevalier, M.; Guillemin, J.-C.; Turowski, M.; Custer, T.; Crépin, C. Cryogenic Photochemical Synthesis and Electronic Spectroscopy of Cyanotetracetylene. *J. Phys. Chem. A* **2017**, *121*, 7374–7384. [CrossRef] [PubMed]
25. Szczepaniak, U.; Ozaki, K.; Tanaka, K.; Ohnishi, Y.; Wada, Y.; Guillemin, J.C.; Crépin, C.; Kołos, R.; Morisawa, Y.; Suzuki, H.; et al. Phosphorescence Excitation Mapping and Vibrational Spectroscopy of HC_9N and $HC_{11}N$ Cyanopolyynes in Organic Solvents. *J. Mol. Struct.* **2020**, *1214*, 128201. [CrossRef]
26. Turowski, M.; Crépin, C.; Couturier-Tamburelli, I.; Pietri, N.; Kołos, R. Low-Temperature Phosphorescence of Dicyanoacetylene in Rare Gas Solids. *Low Temp. Phys.* **2012**, *38*, 723–726. [CrossRef]
27. Crépin, C.; Turowski, M.; Ceponkus, J.; Douin, S.; Boyé-Péronne, S.; Gronowski, M.; Kołos, R. UV-Induced Growth of Cyanopolyyne Chains in Cryogenic Solids. *Phys. Chem. Chem. Phys.* **2011**, *13*, 16780–16785. [CrossRef]
28. Turowski, M.; Crépin, C.; Douin, S.; Kołos, R. Formation and Spectroscopy of Dicyanotriacetylene (NC_8N) in Solid Kr. *J. Phys. Chem. A* **2015**, *119*, 2701–2708. [CrossRef]
29. Szczepaniak, U. Spectroscopy and Photochemistry of Astrophysically-Relevant Molecules of the Cyanoactylene Family. Ph.D. Thesis, Institute of Physical Chemistry, Polish Academy of Sciences, Warsaw, Poland, Université Paris-Saclay, Université Paris-Sud-Paris XI, Orsay, France, 2017. Available online: https://tel.archives-ouvertes.fr/tel-01562041/ (accessed on 1 February 2022).
30. Wright, M.R.; Frosch, R.P.; Robinson, G.W. Phosphorescence Lifetime of Benzene. an Intermolecular Heavy-Atom Effect, a Deuterium Effect, and a Temperature Effect. *J. Chem. Phys.* **1960**, *33*, 934–935. [CrossRef]
31. Minaev, B.F. External Heavy-Atom Effects on Radiative Singlet-Triplet Transitions. *J. Appl. Spectrosc.* **1985**, *43*, 887–890. [CrossRef]
32. Minaev, B. Theoretical Study of the External Heavy Atom Effect on Phosphorescence of Free-Base Porphin Molecule. *Spectrochim. Acta-Part A Mol. Biomol. Spectrosc.* **2004**, *60*, 3213–3224. [CrossRef] [PubMed]
33. Baryshnikov, G.; Minaev, B.; Ågren, H. Theory and Calculation of the Phosphorescence Phenomenon. *Chem. Rev.* **2017**, *117*, 6500–6537. [CrossRef] [PubMed]

34. Turowski, M.; Gronowski, M.; Guillemin, J.C.; Kołos, R. Generation of H-Kr-C_5N and H-Xe-C_5N Molecules. *J. Mol. Struct.* **2012**, *1025*, 140–146. [CrossRef]
35. Kunttu, H.M.; Seetula, J.A. Photogeneration of Ionic Species in Ar, Kr and Xe Matrices Doped with HCl, HBr and HI. *Chem. Phys.* **1994**, *189*, 273–292. [CrossRef]